Additional Hydrogen Bonds and Base-Pair Kinetics in the Symmetrical AMP-DNA Aptamer Complex

Sylvie Nonin-Lecomte, Chin H. Lin, and Dinshaw J. Patel
Cellular Biochemistry and Biophysics Program, Memorial Sloan-Kettering Cancer Center, New York, New York 10021 USA

ABSTRACT The solution structure of an adenosine monophosphate (AMP)-DNA aptamer complex has been determined previously [Lin, C. H., and Patel, D.J. (1997) *Chem. Biol.* 4:817–832]. On a symmetrical aptamer complex containing the same binding loop, but with better resolved spectra, we have identified two additional hydrogen bond-mediated associations in the binding loop. One of these involves a rapidly exchanging G imino proton. The phosphate group of the AMP ligand was identified as the acceptor by comparison with other aptamer complexes. Imino proton exchange measurements also yielded the dissociation constants of the stem and binding loop base pairs. This study shows that nuclear magnetic resonance-based imino proton exchange is a good probe for detection of weak hydrogen-bond associations.

INTRODUCTION

Adenosine monophosphate (AMP) is a universal cofactor which interacts with both proteins and nucleic acids. In vitro selection approaches have defined high-affinity binding sites for AMP on both RNA (Sassanfar and Szostak, 1993) and DNA (Huizenga and Szostak, 1995) aptamers. Our interest has focused on the architecture and hydrogen exchange characteristics of the nucleic acid binding sites and the similarities and differences associated with RNA versus DNA targets. Despite differences in the binding-site sequence, in the secondary and tertiary folds, and in the binding stoichiometry (Jiang et al., 1996; Dieckmann et al., 1996; Lin and Patel, 1997) (1 AMP:1 and 2 AMP:1 for the RNA and DNA complexes, respectively), the RNA and DNA aptamer complexes exhibit similar recognition features in the binding pocket (Fig. 1). This suggests that AMP could be accommodated by a finite set of nucleic acid binding pocket architectures and, in turn, could help in the rational design of binding pockets for the other nucleoside monophosphates. In both cases, the AMP molecule is recognized through the formation of the same G·AMP mismatch alignment, involving the Watson-Crick side of AMP and the minor groove edge of guanine, stacked on a reversed Hoogsteen G·G base pair in one direction and on an adenine in the other. We previously showed that the mismatches in the internal binding loop are as stable as the internal Watson-Crick base pairs in the flanking stems in the AMP-RNA complex (Nonin et al., 1997a). We report here on the kinetics of base-pair opening in the AMP-DNA aptamer complex.

Nuclear magnetic resonance (NMR)-based hydrogen exchange measurements of imino protons provide important complements to the structure information, for example the lifetimes and the dissociation constants of the Watson-Crick and mismatched base pairs (Guéron and Leroy, 1995). The strength of the method relies on its ability to probe the structure at the nucleotide level independently of the knowledge of the folding topology, and to indicate whether an imino proton is protected from exchange with water or not. For example, base pair-hydrogen bonding (H-bonding) can be easily detected because the imino proton exchange is catalyzed by the nitrogen to which it is paired. This process, called intrinsic catalysis, has a characteristic signature in the exchange time measurements versus pH. We have shown in a previous study carried out on the AMP-RNA aptamer complex that it also occurs for imino protons when they are H-bonded to another intrinsic acceptor, such as phosphate group (Nonin et al., 1997a). Thus, we identified four additional H-bonds in the AMP-RNA aptamer complex structure.

The AMP-DNA aptamer complex, whose solution structure has been determined previously (Lin and Patel, 1997), is built from a single-stranded 27-mer DNA aptamer. Its imino proton spectrum is not sufficiently resolved for reliable imino proton exchange measurements. Therefore, a symmetrical self-complementary 14-mer DNA with the same binding pocket was devised (Lin and Patel, 1997; Fig. 1 *a*). Its spectra indicate a similar structure of the binding pocket (Lin, personal results). The 14-mer contains two symmetrical ligand-binding sites. We focus here on this symmetrical aptamer complex. In the absence of ligand, the binding loop imino protons appear as a broad set of resonances, ranging from 9.5 to 11 ppm. With 2 equivalents (eq) AMP, all the imino proton resonances are resolved except for that of the G6 imino proton, whose resonance is too broad to be observed in these conditions, because of fast exchange. (This is also the case for its homolog in the 27-mer complex). The G6 residue is important because it is part of a reverse Hoogsteen pair that closes the binding loop from one side. Deciding whether a fast exchanging proton is H-bonded or not is not straightforward because the large line width may inhibit to detection of nuclear overhauser enhancement spectroscopy (NOESY) or heteronuclear J-coupling crosspeaks. We have applied the same methods as

Received for publication 30 April 2001 and in final form 2 August 2001.
Address reprint requests to Sylvie Nonin-Lecomte, BIOP/PMC-Ecole Polytechnique, 91129 Palaiseau, France. Tel.: 33-1-6933-4413; Fax: 33-1-6933-3004; E-mail: sn@pmcsun1.polytechnique.fr.
© 2001 by the Biophysical Society
0006-3495/01/12/3422/10 $2.00

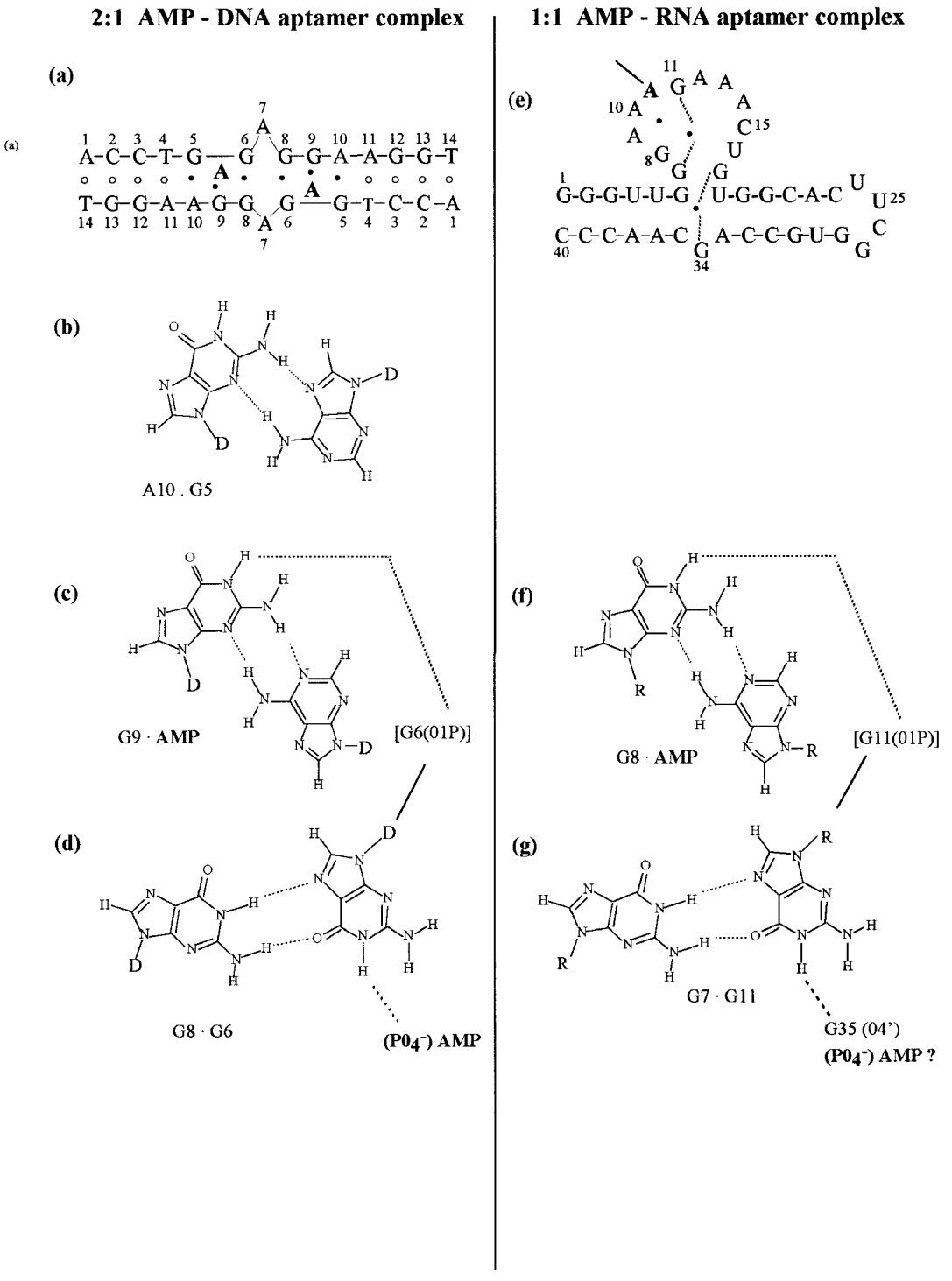

FIGURE 1 Comparison of the sequence and numbering systems of the self-complementary 14-mer G6-DNA (*a*) and of the 40-mer RNA (*e*) AMP aptamers. In both the DNA and the RNA structures, the recognition of AMP involves stacking of purines and formation of a G·AMP mismatch (i.e., G9·AMP in the 14-mer DNA complex (*c*) and G8·AMP in the RNA complex (*f*)). The Watson-Crick edge of AMP binds to the minor groove edge of the guanine. In both structures, the G·AMP mismatch is stacked on a reversed Hoogsteen G·G mismatch pair in one direction (G8·G6 (*d*) in the 14-mer DNA aptamer complex, and G7·G11 (*g*) in the RNA aptamer complex, respectively), and on an adenine in the other. In the DNA aptamer complex, this adenine is engaged in a sheared G·A mismatch alignment (*b*). The additional H-bonds identified in this study are G9 H1—G6 O1P (*c*), and G6 H1—AMP (PO_4^-) (*d*).

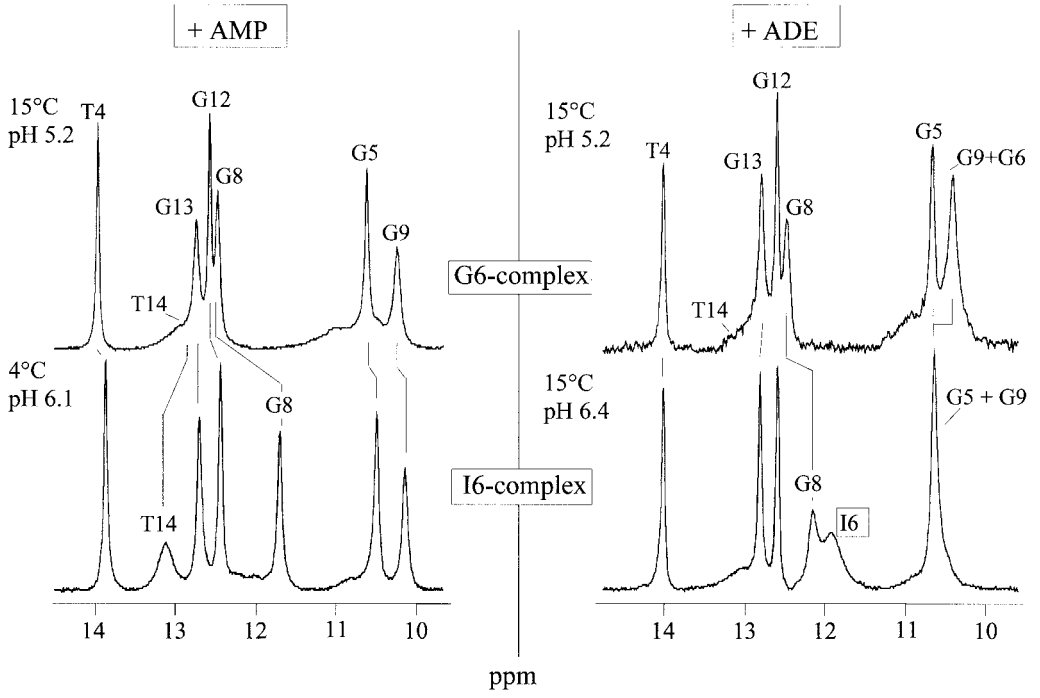

FIGURE 2 400 MHz imino proton spectra recorded in 95% H_2O/5% D_2O; 200 mM KCl and 2 mM EDTA solutions of the G6-DNA (*upper panels*) and I6-DNA (*lower panels*) complexed with AMP (*left panels*) or adenosine (*right panels*). (*a*) Spectrum recorded at pH 5.15 with 4 eq AMP. All the internal Watson-Crick imino proton peaks (T4, G13, and G12) are sharp and resolved. The T14 imino proton of the poorly stable terminal base pair is broadened out by exchange with water. The binding loop imino protons G8, G5, and G9 are resolved and somewhat broadened to different extents. The G6 imino proton is not observed under these conditions. (*b*) Same pH conditions as *a* with 4 eq adenosine. The overall spectrum is unchanged when AMP is replaced by adenosine, except for the former G9 resonance, whose area is doubled. The new unresolved resonance is ascribed to G6 imino proton. In presence of AMP, when G6 is substituted by I6, the resonance is still missing even when the temperature is lowered to 4°C (*spectrum c*). Conversely, in presence of adenosine and at 15°C, the I6 resonance is clearly seen at ~12.1 ppm. This shows that, in the DNA complexes, exchange of G6 or I6 imino protons is catalyzed by the phosphate group of the AMP ligand.

in a previous study of the fast exchanging terminal imino protons (Nonin et al., 1995) to investigate the G6 imino proton in the DNA aptamer complex.

The logic of the paper is as follows. We investigate imino proton exchange in the AMP DNA-aptamer complex, but not in the free aptamer whose imino protons are not resolved. First, we deal with the stem imino protons whose exchange properties will be used as the reference for subsequent analysis of the mismatched base pairs. We then explore the binding site imino protons. To assess the influence of the phosphate group of the AMP ligands on the imino proton exchange kinetics and on complexation, we measured the exchange kinetics in the adenosine-DNA aptamer complex, in which the G6 imino proton peak is observed (Fig. 2). An inosine-substituted DNA aptamer complex (referred to as the I6-complex, its G6 counterpart being similarly referred to as the G6-complex) allowed us to monitor the imino proton exchange of the sixth nucleotide. We thus identify two additional H-bond–mediated associations within the binding loop. These results are applied to the comparison of base-pair kinetics in the complexes of AMP with the DNA and RNA aptamers.

MATERIALS AND METHODS

Oligodeoxynucleotides and NMR sample preparation

The 14-mer and 27-mer DNA aptamers were synthesized and purified as described in the solution structure paper (Lin and Patel, 1997). The [^{17}O]water (45–49.9% ^{17}O enrichment, catalog #87–700-30–8) was purchased from Isotec Inc. (Miamisburg, OH). Oxygen-17 was then regiospecifically incorporated during the chemical synthesis into the anionic oxygen of the G5-G6 phosphate group of the 14-mer DNA aptamer by selective oxidation of the appropriate phosphite intermediate with 0.1 M oxidizing solution, which consists of a mixture of iodine, 1g of [^{17}O]water, 10 ml of pyridine, and 40 ml of tetrahydrofuran. The C3 spacer dimer was synthesized using the C3 spacer phosphoramidite. The C3 spacer, the Dspacer, and the dA-5′-CE phosphoramidite were purchased from Glen Research (Sterling, VA). All samples were dialyzed several times against water. They are phosphate-free, with the exception of the spectrum of Fig. 4. After lyophilization they were dissolved in 95% H_2O/5% D_2O solutions with EDTA 2mM. The stoichiometry of the DNA aptamer complexes was monitored and checked by one-dimensional (1-D) NMR spectra. The pH was measured at room temperature using a calibrated PMH82 Radiometer pH-meter and adjusted using 0.01–0.1 M NaOH and HCl solutions.

NMR spectroscopy

All experiments were performed on a Varian Unity Plus 400 MHz NMR spectrometer (Varian Inc., Palo Alto, CA), except for the spectra of Fig. 3,

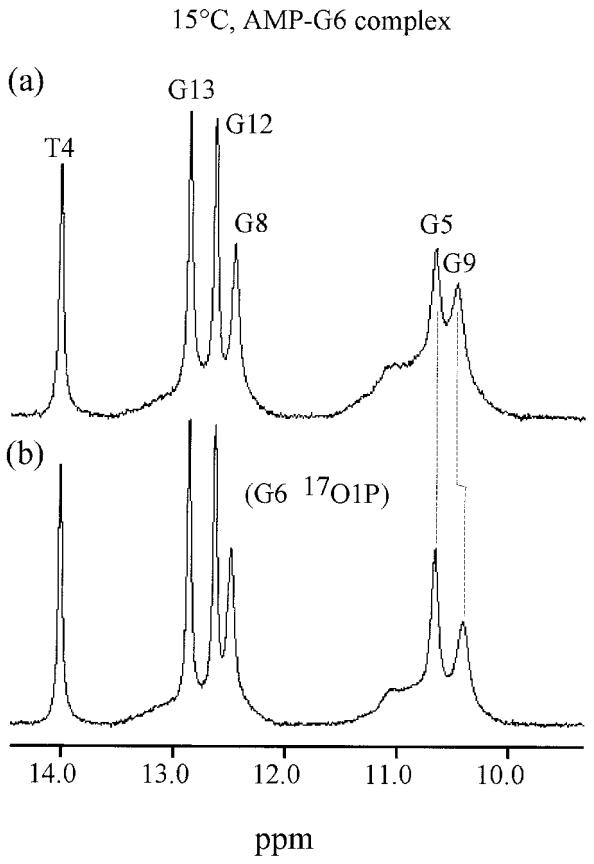

FIGURE 3 600 MHz 1-D NMR spectra in 90% H_2O/10% D_2O of the imino proton region of (*a*) the unlabeled and (*b*) the ^{17}O-labeled 14-mer DNA aptamer-AMP complexes, recorded at 15°C and pH 6.75. The ^{17}O-labeling of G6 O1P produces an upfield shift of the G9 imino proton attributable to the CSA effect, disclosing the proximity of these two positions.

which were recorded on a Varian Plus 600 MHz NMR spectrometer. Proton exchange times and base-pair dissociation constants were determined as described previously (Nonin et al., 1997a), mainly by saturation transfer from water (Forsèn and Hoffman, 1963; Guéron and Leroy, 1995).

Imino proton exchange

We briefly review the basics of imino proton exchange theory (Guéron and Leroy, 1995) required for this work. A more detailed description of the kinetics and the corresponding equations is available as supplementary materials. Similar annotations and equations as described before (Nonin et al., 1996, 1997a) are used. Two cases are distinguished: that of the mononucleosides, and that of the H-bonded imino protons (this includes the cases of base pairs and of imino protons H-bonded to any proton acceptor in the structure).

Three exchange processes can be distinguished for the mononucleosides. At high pH, the exchange rate (k_{ex}) is proportional to the hydroxide concentration (referred to as the N_{OH^-} process or hydroxide catalysis). At lower pH, this process becomes inefficient, and pH-independent catalysis by water (N_{H_2O} process) dominates. The corresponding exchange rate depends only on the imino proton nitrogen (N^1 for guanosine or N^3 for thymidine) pKi. At yet lower pH, the H_2O-catalyzed exchange is accelerated because of protonation of the guanosine N^7 position which lowers the pK of nitrogen N^1 (P_{H_2O} process, where P stands for protonated, or acid catalysis). This process is observed for G but not for T, which lacks a protonation site with pK >0.

Exchange of an H-bonded imino proton requires H-bond disruption. Therefore, the exchange time cannot be smaller than the lifetime τ_0 of the H-bond (in the case of a base pair, τ_0 is the base-pair lifetime). In the open state, the N_{OH^-}, N_{H_2O}, and P_{H_2O} processes contribute as in the mononucleoside, and they are described by the same equations except for a constant α, generally close to 1, that encompasses any difference between the monomer and the open state. The acceptor of the H-bond provides for an additional catalytic process (intrinsic catalysis; N_{int} and P_{int} processes, N and P indicating the protonation state of the base as for N_{H_2O} and P_{H_2O}), which is typically more efficient than the exchange catalysis by the N_{H_2O} and P_{H_2O} processes, because the pK of the intrinsic acceptor is higher than that of water. The N_{int} and P_{int} processes are pH-independent. In other words, the plot of the exchange time versus pH of an imino proton H-bonded with an intrinsic acceptor displays a pH-independent plateau. For weak associations, these processes yield exchange times smaller than that of the corresponding mononucleoside at the same pH.

The imino proton exchange time is:

$$\tau_{ex} = \tau_0 + 1/(K_d \times k_{ex,open}) \quad (1)$$

where $\tau_{ex} = 1/k_{ex}$ is the exchange time experimentally measured, $k_{ex,open}$ the exchange rate from the open state, and K_d the dissociation constant. When τ_{ex} is long compared with the base-pair lifetime τ_0, it is expressed as:

$$\tau_{ex} \approx 1/(K_d \times k_{ex,open}) \quad (2)$$

At basic pH, when N_{OH^-} is the driving exchange process, Eq. 2 becomes:

$$\begin{aligned}\tau_{ex} &\approx 1/(K_d \times k_{ex,open,OH^-}) \\ &= 1/(K_d \times \alpha k_{ex,OH^-}) \\ &= \tau_{ex,OH^-}/(\alpha K_d) \end{aligned} \quad (3)$$

αK_d is called the apparent dissociation constant and is experimentally obtained by comparison of the N_{OH^-} catalysis curves in the monomer ($\tau_{ex,OH^-} = 1/k_{ex,OH^-}$) and in the H-bonded nucleotide (τ_{ex}). It is replaced by a protection factor (pf) when the experimental imino proton curve is only displaced by a small factor compared with the monomer over the entire pH range.

RESULTS

1-D NMR spectra

The 1-D NMR spectrum of the AMP-G6-complex, recorded in water at 15°C and pH 5.15 (the pH at which the imino proton exchange of guanosine is the slowest), exhibits the four imino proton resonances expected for the stem Watson-Crick base pairs between 12.5 and 14.5 ppm (Fig. 2, *upper left panel*). In the binding loop, G8, G5, and G9 imino proton peaks are clearly observable and broadened somewhat to different extents. The G8 imino proton resonates downfield of 12 ppm, whereas the G5 and G9 imino protons are upfield shifted between 10 and 11 ppm. The G6 imino proton is not observed. The G9 imino proton resonance is the only one which shows a chemical shift anisotropy (CSA) effect when G6 O1P is O^{17}-labeled (Fig. 3).

To assess the catalytic effect of the AMP phosphate group on the binding site imino protons, we replaced AMP

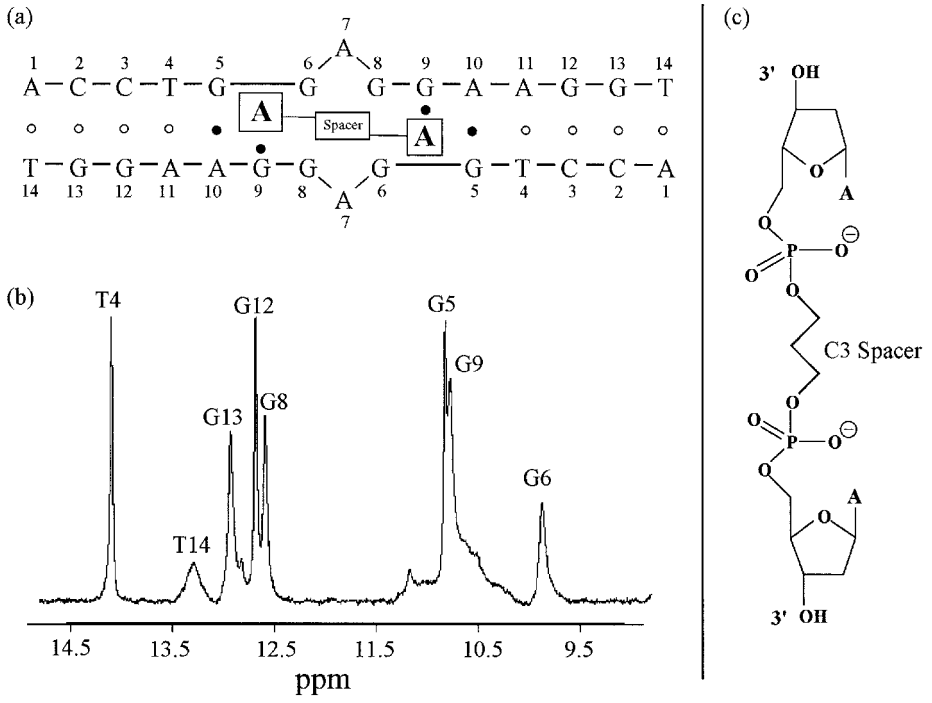

FIGURE 4 (*a*) Sequence and numbering system of the 14-mer G6-DNA aptamer complexed with one eq of the C3 spacer (*c*). (*b*) 400 MHz imino proton spectrum recorded in 90% H_2O/10% D_2O, 50 mM KCl, and 10 mM phosphate-buffered solution of the 1:1 C3 spacer/G6/DNA complex at pH 6.40 and 4°C. The G6 imino proton resonance reappears upfield at ~9.8 ppm.

by adenosine after extensive dialysis of the AMP 14-mer DNA aptamer complex against water. The imino proton region is very similar to that of the AMP-DNA aptamer complex (Fig. 2, *upper right panel*) and is unchanged upon addition of excess adenosine. The main difference between the two spectra is the area of the G9 imino proton peak, which approximately doubles in intensity in the adenosine-DNA aptamer complex. The extra resonance, tentatively assigned to G6, is not resolved from G9 at 15°C and poorly resolved at 4°C (data not shown).

The assignment of G6 is confirmed by the use of an inosine I6-DNA analog, devised to shift the imino proton of the sixth nucleotide downfield. In the adenosine-I6-complex, the I6 imino proton peak is resolved at 11.9 ppm (Fig. 2, *lower right panel*). The remainder of the imino proton region is very similar to that of the G6-complex, except for the imino proton resonance of G8, which is shifted upfield. The I6 imino resonance is still unobserved in the AMP-I6-complex (Fig. 2, *lower left panel*), but reappears when the G6-DNA is complexed with the C3 spacer, in which two AMP nucleotides are linked by their 5′-end through a propane spacer (Fig. 4).

Exchange of the stem imino protons

We have measured the exchange times of T4, G12, and G13 imino protons versus pH in the AMP-G6-, adenosine-G6-, and adenosine-I6-complexes (Fig. 5, *upper*, *middle*, and *lower left panels*, respectively). The exchange times measured for 2 and 4 eq of AMP or adenosine (not shown) on the G6-complex are the same. The addition of an excess of ligand drives the equilibrium toward the formation of the complex (mass action law). The fact that the exchange times are unchanged by excess of ligands, even for the more stable base pairs, proves that the dissociation of the complex is not part of the imino proton exchange process. The terminal T14 imino proton resonance at 13.2 ppm is broadened by exchanging with water at 15°C. We did not monitor the kinetics of this proton in this study.

The pH-dependent behavior is similar to what is commonly observed for Watson-Crick base pairs and the exchange times are unaffected by the nature of the ligand and the sixth nucleotide. The N_{OH^-} process of the base-paired T4, G12, and G13 imino protons is less efficient than that of the corresponding monomer (i.e., the exchange times are slower). According to Eq. 2, the exchange is slowed down by a factor which yields the apparent dissociation constant of the base (αK_d). The apparent dissociation constants ranging from 10^{-4} to 5×10^{-3} are listed in Table 1. The pH-independent N_{int} process characteristic of H-bonded imino protons is seen ~pH 6.5 for the three imino protons. The proton acceptors for T4, G12, and G13 at the plateau are nitrogens N^1 of A11, N^3 of C3, and N^3 of C2, respectively, across the Watson-Crick T4·A11, C3·G12, and C2·G13 base pairs. The shortening of the exchange times measured for G13 and G12 below pH 6 reflects contributions from the P_{int}

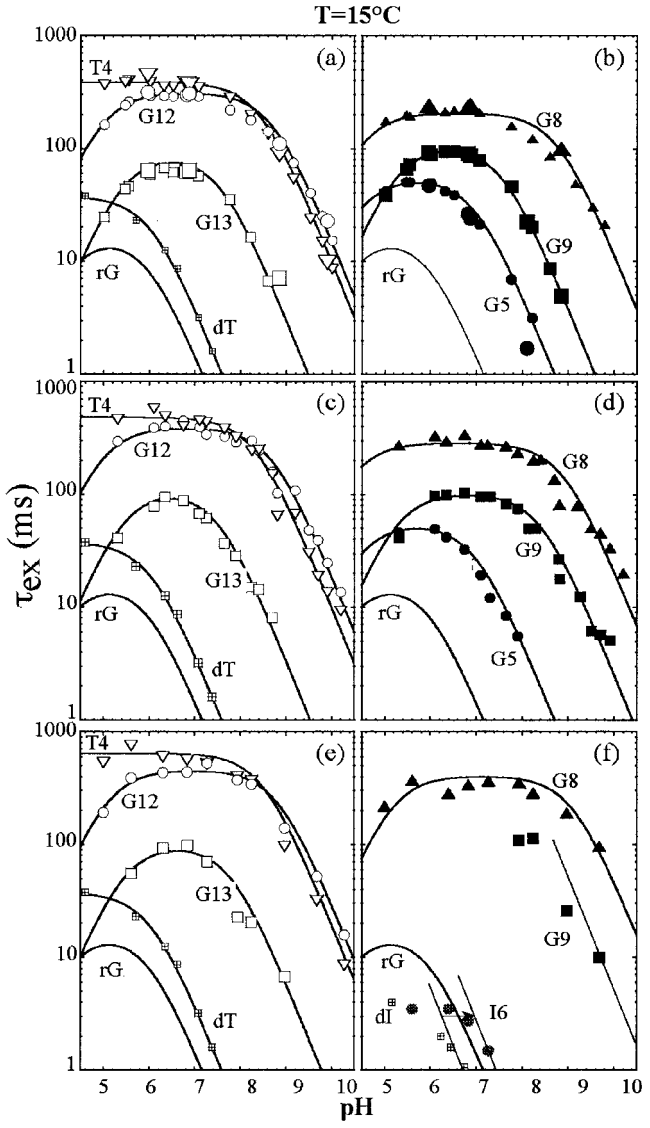

FIGURE 5 Watson-Crick stem imino proton (*left panels*, open symbols) and binding loop imino proton (*right panels*, filled symbols) exchange times measured versus pH at 15°C in the DNA complexed with 2 eq of either AMP or adenosine. The experimental data were fitted using the usual equations (Nonin et al., 1996). The rG curve displayed in all panels is that from the RNA aptamer study (Nonin et al., 1997a). (*a*, *b*) G6-DNA complexed with 2 eq or 4 eq (enlarged symbols) of AMP. The exchange kinetics of the binding loop imino protons (G8, ▲; G9, ■; and G5, ●) is similar to that of G12 and G13, showing that G8 and G9 are engaged in stable base pairs. The differences observed between the G5 and rG curves are ascribed to a pf. At pH 8, G5 imino proton exchange is catalyzed by the phosphate of the ligand in excess (enlarged ●). (*c*, *d*) Same symbols as *a* and *b*, respectively, for the G6-DNA complexed with 2 eq adenosine. (*e*, *f*) Titration curves for the I6-DNA complexed with 2 eq adenosine. The exchange kinetics of the stem Watson-Crick imino protons and of G9 and G8 are similar as in the G6 complex. G9 data were collected only above pH 8 where G5 imino proton is broadened out by exchange with OH^-, because G9 and G5 NMR imino proton lines are not resolved in this complex (Fig. 2). I6 imino proton (*f*, ▨) exchanges roughly similar to dI imino proton (□) and the slight N_{OH^-} discrepancy observed between the two curves is ascribed to a small pf of 0.19.

TABLE 1 Apparent dissociation constants (αK_d) and protection factors (pf) at 15°C for the G6-DNA and I6-DNA aptamer complexes

Base number	αK_d or pf G6 DNA-AMP	αK_d or pf G6 DNA-ADE	αK_d or pf I6 DNA-ADE
T4	4×10^{-4}	4×10^{-4}	2×10^{-4}
G13	5×10^{-3}	4.5×10^{-3}	2.5×10^{-3}
G12	1×10^{-4}	0.8×10^{-4}	0.5×10^{-4}
G8	1.3×10^{-4}	0.5×10^{-4}	0.2×10^{-4}
G5	3×10^{-2} (pf)	3.2×10^{-2} (pf)	
G9	4×10^{-3}	6×10^{-4}	$\approx 5 \times 10^{-4}$
G6/I6			≈ 0.19 (pf)

Unless otherwise stated, these values correspond to αK_d.

process attributable to a small fraction of N^7-protonated guanosines.

Exchange of the binding site imino protons

The exchange time measurements for G5, G8, and G9 follow kinetics similar to those of G13 and G12 (Fig. 5, *b*, *d*, *f*). The N_{OH^-} process is the driving exchange process above pH 7.5 for G5 and G9, and above pH 9 for G8. The comparison of the N_{OH^-} process for these imino protons and that of the monomer according to Eq. 2, yields the ratios listed in Table 1. They range from 1.3×10^{-4} to 3×10^{-2}. The exchange kinetics of the G5, G9, and G/I6 imino protons depends upon the presence or absence of the ligand phosphate group. Conversely to G9, G5 imino proton exchange is catalyzed by the phosphate group of AMP present in excess at pH $\approx$ 8 (Fig. 5 *b*, enlarged circle). G6 and I6 imino protons exchange faster in the AMP-complexes than their homologs of rG and dI monomers.

DISCUSSION

Stem imino protons

All the stem imino proton exchange features (Fig. 5 *c*), as well as the apparent dissociation constants (Table 1), are unaffected upon replacing AMP by adenosine, as expected because these protons are far from the two AMP ligands in the structure. Their αK_d also fall in the range of what is commonly observed on DNA for second and third stem base pairs starting from the ends, i.e., 10^{-2} to 10^{-4} (Guéron et al., 1990; Guéron and Leroy, 1992, 1995; Nonin et al., 1995).

The very fast exchange of the G6 imino proton with water is catalyzed by the AMP phosphate group

We have monitored the imino proton exchange times of the AMP and adenosine I6-complexes versus pH (Fig. 5, *e* and *f*). The apparent dissociation constants (Table 1) show that

the inosine substitution does not perturb the base-pair stability in the stem and in the binding site. The similarity of the exchange characteristics of I6 and dI monomer imino protons shows that, in the absence of ligand phosphate groups, the I6 imino proton exchange is not catalyzed. I6 imino proton is thus not H-bonded in the complex. The small pf (0.19) observed in the adenosine-I6-complex for the N_{OH^-} process (Fig. 5 *f*) probably arises from the fact that I6 lies in the core of the binding loop. Because the G6 and I6 imino proton peaks disappear in the AMP complexes (Fig. 2), the exchange process takes place as if the effective concentration of catalyst (i.e., of AMP phosphate group) seen by these imino protons was high, and/or the catalyst was permanently maintained close to these protons via H-bonds. At pH 5.15, rG and dI imino protons exchange in the range of a few milliseconds (cf. Fig. 5) and their resonances are seen on a 1-D spectrum. The fact that the G6 and I6 imino protons exchange faster in the AMP-complexes than in the monomer controls (G6 and I6 imino proton peaks are broadened out to baseline by exchange at pH 5.15) is characteristic of the intrinsic catalysis for weak base pairs or associations. The qualification "intrinsic" applies in this case, as AMP is part of the complex. In weak intrinsic associations, of which terminal base pairs provide good examples, the apparent dissociation constant or the pf is high, and consequently, the efficiency of the N_{H_2O} process is more or less the same as for the monomer. However, the N_{int} process is much more efficient because pK_{int} of the intrinsic bond acceptor is much higher than that of water (-1.7); it is all the more efficient because it is not slowed down by a small dissociation constant. Thus, the combination of a high dissociation constant or pf and intrinsic catalysis results in an exchange faster than from the monomer. This feature has been seen before for the Watson-Crick terminal base pairs (Nonin et al., 1995) and for the pseudo-AT base pairs of the TTTA tetra loops of the *i*-motif structure formed by d(C-CTTTACC) (Nonin et al., 1997b). G6 and I6 imino protons are exchange-catalyzed by the AMP phosphate group in a N_{int}-like process and are sensing the phosphate group through H-bonding. This implies that the phosphate group has moved toward I6 imino proton at least part of the time. In the C3 spacer-G6 complex (Fig. 4 *a*), in which two AMP nucleotides are linked on their 5′-end by a propane spacer (Fig. 4 *c*), the pK of the two AMP phosphate groups is decreased by ~4 units. The catalysis is thus ~10,000 times less efficient than by the terminal phosphate of the AMP. As expected, G6 imino resonance reappears (Fig. 4 *b*). The fact that it is upfield shifted to ~9.8 ppm indicates an interaction with a phosphate oxygen again.

The binding site imino protons; an additional interstrand H-bond at the G9 imino proton site

The fact that G8 H1 is base-paired (to G6 N^7) in the structure (Lin and Patel, 1997) translates into the presence of a large N_{int} plateau corresponding to exchange times only 20 times larger than from the monomer, i.e., much smaller than that expected from the N_{H_2O} process and the αK_d of $\sim 10^{-4}$ given by the N_{OH^-} process. In contrast, the G5 N_{OH^-} and N_{H_2O} processes are slowed down by the factor within a factor of 10 from the monomer processes, which is consistent with the previous finding that G5 imino proton is not H-bonded in the structure (Fig. 1 *b*). The observation that at pH $\approx$ 8 G5 imino proton exchange is catalyzed by the phosphate groups of AMP present in excess also confirms the exposure to the solvent of this imino proton.

The case of G9 is different. In the AMP and adenosine-DNA complexes, G9 imino proton exchange kinetics are typically those of a H-bonded imino proton with a N_{int} plateau ranging from pH 6 to 7.5 and an apparent dissociation constant of respectively 4×10^{-3} and 6×10^{-4} (Fig. 5 *d*). In both cases, the existence of a pH-independent intrinsic catalysis requires that G9 imino proton must be H-bonded in the complex. Examination of the AMP-DNA complex refined solution structures of lowest energy computed from nuclear Overhauser enhancement (NOE) restraints shows that for each of them, this proton is located 2.1 ± 0.3 Å from G6 O1P of the complementary strand, and that a H-bond is readily accommodated at this site. (Measuring the angle of the potential H-bond has no significance here because the phosphate group positions were not experimentally restrained during simulation). No other potential acceptor emerges within a sphere of 5 Å around the G9 imino proton. The fact that the G9 imino proton is the only resonance to show CSA effect when G6 O1P is O^{17}-labeled (Fig. 3), confirms the existence of an additional base-backbone H-bond between G9 and G6 and the ability of the method to probe for previously unidentified H-bonds. G9 exchange times are insensitive to an excess of AMP, but are raised by almost a factor of 7 when the phosphate group of the ligands is removed. Examination of the refined structures shows that the two AMP phosphate groups are too far from the two G9 for efficient catalysis, and suggests that they indirectly destabilize the G9 base·G6 backbone interaction, which translates into an increase of the αK_d.

Novel features of the AMP-DNA aptamer complex

The AMP-DNA aptamer complex represents the first example of two ligands bound to adjacent sites along the DNA aptamer (Lin and Patel, 1997). As such, the system introduced its own set of challenges for structural characterization by NOE structural and hydrogen exchange kinetics measurements. For instance, the imino proton of G6, adjacent to the ligand recognition site, was very broad in the AMP complex, independent of pH and temperature (Fig. 2, *left panel*). This challenge was overcome in this study by substituting adenosine for AMP at the ligand level and by replacing guanosine by inosine at position 6 at the DNA aptamer level in the complex (Fig. 2, *right panel*). More

decisively, the imino proton of G6 was readily observable in the complex with the two AMP molecules covalently linked through a C3 spacer (Fig. 4). The greater immobilization of the phosphate groups by the C3 linker presumably affected the exchange characteristics of the imino protons of the G6 residues, which is consistent with the proposed H-bond between the imino proton of G6 and the phosphate group of AMP at each of the symmetry-related binding sites.

Newer NMR methods now allow the ready identification of N-H··N H-bonds because of measurable J_{NN} couplings and, to a lesser extent, N-H··O = C H-bonds, because of significantly reduced J_{NC} couplings (Zidek et al., 2001). In contrast, the measurement of N-H hydrogen bonds to phosphate groups remains a considerable challenge. Our use of imino proton hydrogen exchange measurements as a function of ligand type (nucleotide AMP vs. nucleoside adenosine) or backbone modification (O^{17} labeling) has opened up novel approaches for detection and identification of N-H··phosphate H-bonds.

The quantitative base-pair kinetic measurements have also provided insights into the relative stability of base mismatches and base·phosphate interactions compared with standard Watson-Crick base pairs in the core of the AMP-DNA aptamer complex. Strikingly, the imino proton of G8 involved in the reversed G8·G6 mismatch pair and the imino proton of G9 involved in the G9·phosphate interaction, exhibit αK_d values of comparable magnitude, to those for the imino protons of G12 and G13 involved in Watson-Crick G·C pair formation (Table 1). These observations were intuitively unexpected and potentially reflect a compact binding site pocket containing base pairs, mismatches, and base·phosphate interactions of comparable kinetic stability.

Comparison of the DNA and the RNA AMP-aptamer complexes

The exchange studies show that, as in the AMP-RNA aptamer complex, the mismatched pairs of the AMP-binding loop are as stable as the internal Watson-Crick base pairs of the flanking helical stems in the AMP-DNA aptamer complex. In the RNA aptamer complex, this is particularly true for the reversed Hoogsteen G7·G11 mismatch on which the G8·AMP pair is stacked, and whose apparent dissociation constant is $\sim 1.5 \times 10^{-5}$ at 15°C (Nonin et al., 1997a). Here, the homolog G8·G6 base pair in the DNA aptamer complex displays an αK_d of $\sim 10^{-4}$, similar to that of the G12·C3 Watson Crick base pairs of the flanking stems. In light of the additional H-bond identified in the DNA aptamer complex between G6 imino and the AMP phosphate group, we found that in the RNA structure, the homolog G11 imino proton, which is most probably H-bonded to G35 O4′, can also be approached by the AMP phosphate group. Such interaction would enhance the similarity of the RNA and DNA binding loops (Fig. 1). The exchange kinetics of the two G imino protons paired with the AMP ligand, G8 for the RNA aptamer complex (Jiang et al., 1996; Dieckmann et al., 1996) and G9 for the DNA aptamer complex, identifies an additional H-bond between these protons and one neighboring phosphate group oxygen of the backbone, and gave a corresponding apparent dissociation constant of $\sim 10^{-4}$ at 15°C for both. In both cases, the binding loop stability reflects the stacking of the purines and the extensive intra-loop H-bond network that leaves almost no imino proton freely exposed to the solvent.

CONCLUSION

NMR methods have contributed to our current understanding of the architecture and adaptability of nucleic acid binding pockets in complexes with ligands ranging from cofactors to amino acids, saccharides, peptides, and proteins (Hermann and Patel, 2000). The majority of this information is deduced from an analysis of intermolecular NOE data, which can be translated into alignment patterns at the intermolecular interface. More recently, the implementation of new pulse sequences for the observation of heteronuclear J-coupling across H-bonds in nucleic acids have proven to be very helpful in structure determination because they provide for the direct identification of the H-bond acceptor (Dingley et al., 2000; Majumdar et al., 1999). These 2-D methods often require labeling (for example, ^{15}N labeling for observation $^{2}J_{NN}$ couplings observation).

The AMP-DNA aptamer complex contains many unusual features associated with the binding of two equivalents of AMP within the distorted minor groove of a zippered-up internal loop segment (Lin and Patel, 1997). Zippering up involves reversed Hoogsteen G·G, sheared G·A, and G·AMP mismatches, with distinct purine base edges for alignment (Fig. 1). The guanine imino protons within the zippered-up segment are either H-bonded across the mismatch pairs or, as shown in the present study using imino proton exchange and base kinetics, can H-bond to either backbone phosphate oxygens or the phosphate group of the bound AMP. The binding pocket is defined by this network of stacking and pairing alignments, with these elements also contributing to molecular recognition and discrimination. Adaptive recognition, as observed in the AMP-DNA aptamer complex, and reported previously for cofactor, amino acid, and peptide complexes with DNA and RNA aptamers, could emerge as a critical modulator of biological function. Our previous studies of the AMP-RNA aptamer complex (Nonin et al., 1997) and the present study on the AMP-DNA aptamer complex demonstrate that hydrogen exchange is an ideal probe for quantitatively monitoring adaptive recognition at the individual base residue in nucleic acid complexes.

The study of the exchange kinetics of the AMP-DNA aptamer complex has yielded information on the base-

pair stability and identified two additional H-bonds in the binding loop. It has also been shown that in nucleic acids, the imino proton hydrogen exchange measurement is a very simple method relying on 1-D experiments which can rapidly provide complementary information related to the accessibility and H-bonding potential, even in cases of rapidly exchanging imino protons. The use of the three approaches (NOE, hetero J-coupling, imino proton exchange) helps to overcome uncertainties where they occur.

SUPPLEMENTARY MATERIALS

The significance of the imino proton exchange time measurements

The imino proton exchange theory has been extensively described (Guéron and Leroy, 1995). Similar annotations and equations as described before are used (Nonin et al., 1996, 1997a). We recall that two cases must be distinguished: that of the mononucleosides and that of H-bonded imino protons (this includes the cases of base pairs and of imino protons H-bonded to whatever proton acceptor in the structure).

Three processes can be distinguished on the monomer. At high pHs, the exchange rate (k_{ex}) is proportional to the hydroxide concentration (Eq. 1, process referred to as the N_{OH^-} process or hydroxide catalysis). Then, as the pH is lowered, the exchange becomes catalyzed by water (N_{H_2O} process). The corresponding exchange rate is pH-independent and depends only on the imino proton nitrogen pK*i* (Eq. 2). At lower pHs, the exchange is accelerated because of protonation of the guanosine N^7 position which lowers the pK of nitrogen N^1 (Eq. 3, P_{H_2O} process in which P stands for protonated, or acid catalysis). The proton acceptor is again water. This latter process is not observed on dT because no position on this pyrimidine ring protonates above pH 0.

$$k_{ex,OH^-} = q_{OH^-}10^{pH-pKi} \quad (1)$$

$$k_{ex,H_2O} = q_{H_2O}10^{-pKi} \quad (2)$$

$$k'_{ex,H_2O} = q_{H_2O}10^{-pK'i} \quad (3)$$

where q_{OH^-} and q_{H_2O} are respectively collision and pseudocollision constants, and pK*i* and pK′*i* the imino position pKs of the neutral and the protonated mononucleoside. The resulting exchange rate is then:

$$k_{ex} = fk'_{ex,H_2O} + (1 - f)(k_{ex,H_2O} + k_{ex,OH^-}) \quad (4)$$

where f is the fraction of protonated mononucleoside. The mononucleoside exchange time τ_{ex} is defined as the reciprocal of k_{ex}.

$$\tau_{ex} = 1/k_{ex} \quad (5)$$

Imino proton exchange from a base pair or a H-bonded state was shown so far to always require initial base-pair opening or H-bond disruption. The N_{OH^-}, N_{H_2O}, and P_{H_2O} processes contribute then similarly in the open state and in the mononucleoside, and are described by the same equations, with the exception of a constant α that encompasses any differences between the monomer and the open state.

$$k_{ex,open,OH^-} = \alpha q_{OH^-}10^{pH-pKi} = \alpha k_{ex,OH^-} \quad (7)$$

$$k_{ex,open,H_2O} = \alpha q_{H_2O}10^{-pKi} = \alpha k_{ex,H_2O} \quad (8)$$

$$k'_{ex,open,H_2O} = \alpha q_{H_2O}10^{-pK'i} = \alpha k'_{ex,H_2O} \quad (9)$$

In most cases $k_{ex,open,H_2O}$ and $k'_{ex,open,H_2O}$ are not efficient, as they are overcome by the intrinsic catalysis process (N_{int} and P_{int}, respectively), a process in which the acceptor is intrinsic to the base pair, and directly or indirectly H-bonded to the imino proton. The N_{int} and P_{int} processes are pH-independent and the resulting exchanging rate may be expressed as follows:

$$k_{ex,open,int} \approx fk'_{int}10^{pKint-pK'i} + (1 - f)k_{int}10^{pKint-pKi} \quad (10)$$

where k_{int} and k'_{int} are pseudocollision constants, and pK_{int} is the pK of the intrinsic acceptor site (i.e., N^3C, N^1A and N^7G in the G·C and A·T Watson-Crick base pairs, and the G·G Hoogsteen base pair, respectively). The overall exchange rate from the open state $k_{ex,open}$ is then approximated by:

$$k_{ex,open} \approx k_{ex,open,int} + (1 - f)k_{ex,open,OH^-} \quad (11)$$

When the imino proton exchange time is long compared with the base pair lifetime τ_0, it is expressed as:

$$\tau_{ex} \approx 1/(K_d k_{ex,open}) \quad (12)$$

This equation is used to fit the experimental data of τ_{ex} versus pH. At basic pH, when N_{OH^-} is the driving exchange process, Eq. 12 simplifies into:

$$\tau_{ex} \approx 1/(K_d k_{ex,open,OH^-}) = 1/(K_d \alpha k_{ex,OH^-}) = \tau_{ex,OH^-}/(\alpha K_d) \quad (13)$$

αK_d is the apparent dissociation constant and is experimentally obtained by comparison of the N_{OH^-} catalysis curves in the monomer and in the H-bonded nucleotide.

We thank Dr. Maurice Guéron for stimulating discussions. Dr. Ali Kettani is acknowledged for providing routines to process the NMR kinetic experiments. D.J.P. was funded by National Institutes of Health CA 46778.

REFERENCES

Dieckmann, T., E. Suzuki, G. K. Nakamura, and J. Feigon. 1996. Solution structure of an ATP-binding RNA aptamer reveals a novel fold. *RNA.* 2:628–640.

Dingley, A. J., J. E. Masse, J. Feigon, and S. Gezesiek. 2000. Characterization of the hydrogen bond network in guanosine quartets by internucleotide $^{3h}J_{NC'}$ and $^{2h}J_{NN}$ scalar couplings. *J. Biomol. NMR.* 16: 279–289.

Forsèn, S., and R. A. Hoffman. 1963. A study of moderately rapid chemical exchange reaction by means of nuclear magnetic double resonance. *J. Chem. Phys.* 39:2892–2901.

Guéron, M., E. Charretier, J. Hagerhorst, M. Kochoyan, J. L. Leroy, and A. Moraillon. 1990. Applications to imino proton exchange to nucleic acid kinetics and structure. *In* Structure and Methods. R. H. Sarma and M. H. Sarma, editors. Adenine Press, Guilderland, New York. 113–137.

Guéron, M., and J. L. Leroy. 1992. Base-pair opening in double-stranded nucleic acids. *In* Nucleic Acids and Molecular Biology. F. Eckstein and D. M. Lilley, editors. Springer-Verlag, Berlin. 1–22.

Guéron, M., and J. L. Leroy. 1995. Studies of base pair kinetics by NMR measurement of proton exchange. *In* Methods in Enzymology. T. D. James, editor. Academic Press, San Diego. 383–413.

Hermann, T., and D. J. Patel. 2000. Adaptive recognition by nucleic acid aptamers. *Science.* 287:820–825.

Huizenga, D. E., and J. W. Szostak. 1995. A DNA aptamer that binds adenosine and ATP. *Biochemistry.* 34:656–665.

Jiang, F., R. A. Kumar, R. A. Jones, and D. J. Patel. 1996. Structural basis of RNA folding and recognition in an AMP-RNA aptamer complex. *Nature.* 382:183–186.

Lin, C. H., and D. J. Patel. 1997. Structural basis of RNA folding and recognition in an AMP-DNA aptamer complex: distinct architectures but common recognition motifs for DNA and RNA aptamers complexed with AMP. *Chem. Biol.* 4:817–832.

Majumdar, A., A. Kettani, and E. Skripkin. 1999. Observation and measurement of internucleotide $^{2}J_{NN}$ coupling constants between ^{15}N nuclei with widely separated chemical shifts. *J. Biomol. NMR.* 14:67–70.

Morris, G. A., and R. Freeman. 1978. Selective excitation techniques in Fourier transform NMR. *J. Magn. Reson.* 29:433–462.

Nonin, S., J. L. Leroy, and M. Guéron. 1995. Terminal base pairs of oligodeoxynucleotides: imino proton exchange and fraying. *Biochemistry.* 34:10652–10659.

Nonin, S., J. L. Leroy, and M. Guéron. 1996. Acid-induced exchange of the imino proton in G·C pairs. *Nucleic Acids Res.* 24:586–595.

Nonin, S., F. Jiang, and D. J. Patel. 1997a. Imino proton exchange and base-pair kinetics in the AMP-RNA aptamer complex. *J. Mol. Biol.* 268:359–374.

Nonin, S., A. T. Phan, and J. L. Leroy. 1997b. Solution structure and base-pair opening kinetics of the *i*-motif dimer of d(5mCCTTTACC): a non-canonical structure with possible roles in chromosome stability. *Structure.* 9:1231–1246.

Plateau, P., and M. Guéron. 1982. Exchangeable protons without base line distortion using a new strong pulse sequence. *J. Am. Chem. Soc.* 104: 7310–7311.

Sassanfar, M., and J. W. Szostak. 1993. An RNA motif that binds AMP. *Nature.* 364:550–553.

Ts'o, P. O. 1974. Basic Principles of Nucleic Acid Chemistry, Vol.1. Academic Press, New York. 462.

Zidek, L., R. Stefl, and V. Sklenar. 2001. NMR methodology for the study of nucleic acids. *Curr. Opin. Struct. Biol.* 11:275–281.